Fuel 216 (2018) 341–348

Contents lists available at ScienceDirect

Fuel

journal homepage: www.elsevier.com/locate/fuel

Full Length Article

FT-ICR MS analysis of blended pine-microalgae feedstock HTL biocrudes

Jacqueline M. Jarvis[a], Justin M. Billing[b], Yuri E. Corilo[c], Andrew J. Schmidt[b], Richard T. Hallen[b], Tanner M. Schaub[a,*]

[a] Chemical Analysis and Instrumentation Laboratory, College of Agricultural, Consumer and Environmental Sciences, New Mexico State University, 945 College Avenue, Las Cruces, NM 88003, USA
[b] Chemical and Biological Processes Development Group, Pacific Northwest National Laboratory, P.O. Box 999, Richland, WA 99352, USA
[c] National High Magnetic Field Laboratory, Florida State University, 1800 East Paul Dirac Drive, Tallahassee, FL 32310-4005, USA

ARTICLE INFO

Keywords:
HTL
Hydrothermal liquefaction
Biocrude
Biomass
FT-ICR
Mass spectrometry

ABSTRACT

Fourier transform ion cyclotron resonance mass spectrometry (FT-ICR MS) is utilized for direct comparison of the chemical composition of biocrudes generated from the hydrothermal liquefaction of 100% pine, 100% algae, 75:25 pine:algae, and 50:50 pine:algae feedstocks. This analysis reveals that the composition of the 72:25 and 50:50 pine:algal HTL biocrudes is essentially a composite of the two parent feeds (i.e., pine and algae) with a lower relative abundance of O_x species and a higher relative abundance of nitrogen-containing species than the pine HTL biocrude. Alternatively, the biocrude blends have a lower relative abundance of nitrogen-containing species where N > 2 than the algal HTL biocrude. The 75:25 pine:algal HTL biocrude has more elemental formulae in common with the pine HTL biocrude than the 50:50 blend; however, both blends have more elemental formulae in common with the algal HTL biocrude. Interestingly, > 20% of the elemental formulae assigned to monoisotopic peaks within the 75:25 and 50:50 biocrude blends are species not present in either the pine or algal HTL biocrudes. The highest relative abundance of these new species belong to the $N_2O_{4\text{-}6}$ classes, which correspond to heteroatom classes with a moderate number of nitrogen atoms and higher number of oxygen atoms per molecules than the species within the pure algal HTL biocrude. Compositionally, the novel species have the same structural motif but are of higher DBE and carbon numbers than the species within the algal HTL biocrude. These original species are most likely generated from reactions between molecules from both feeds, which results in compounds with higher oxygen content than typically seen in the algal HTL biocrude but also higher nitrogen contents than observed in the pine HTL biocrude.

1. Introduction

Hydrothermal liquefaction is an effective process for conversion of wet biomass feedstocks to oil [1–3]. Among feedstock choices, microalgae has been studied as an HTL candidate feed through the recent interest in that material for biofuel development [4–8]. Harvested algal cultures are well-suited as HTL feedstock because they do not require significant sample preparation, can contain relatively high lipid content and additional water is not needed to generate a pumpable slurry [1].

Nonetheless, the availability of algal biomass for biofuel production is limited by seasonal harvest variability (among other cultivation challenges), with higher summer productivity than that of winter [3]. Techno-economic analysis reveals that the under-utilization of equipment during winter results in significant costs penalties for production economics [3]. In fact, feedstock costs limit the viability of commercial-scale HTL biocrude production regardless of feedstock and single biomass sources are not available in sufficient quantity to support a large-scale HTL operation, let alone a cost-effective upgrading unit.

Mixed-biomass HTL addresses feedstock supply limitations and allows for development of regionally significant biomass sources. The use of multiple biomass sources provides a means to tailor feedstock composition to maximize throughput and mitigate production issues. Hydrothermal liquefaction of mixed microalgal species and/or microalgae mixed with other biomass has been shown to improve the economic prospect of HTL operations [9]. Chen et al. generated HTL biocrude from mixed swine mature/algae blends to determine the feasibility of mixed feeds [10]. The abundant nutrients within swine manure were used to enhance the growth of algae and co-liquefaction was determined to be economically advantageous [10]. Brilman et al. studied the co-liquefaction of microalgae, wood, and sugar beet pulp [11]. Similarly, Madsen et al. preformed quantitative analysis on composition of HTL biocrudes from lignocellulosic, macroalgae,

* Corresponding author.
E-mail address: tschaub@nmsu.edu (T.M. Schaub).

https://doi.org/10.1016/j.fuel.2017.12.016
Received 4 August 2017; Received in revised form 29 November 2017; Accepted 4 December 2017
Available online 12 December 2017
0016-2361/ © 2017 Elsevier Ltd. All rights reserved.

microalgae, residues, and mixtures of the later [12]. Results from both studies show that biocrudes generated from mixed lignocellulosic/microalgal feedstocks differed from the calculated values (linear average for neat feeds) and suggest the need for further research on the co-liquefaction of mixed feeds [11,12].

Here, Pacific Northwest National Laboratory (PNNL) has generated several HTL biocrudes from a mixture of pine waste and microalgal feedstocks in variable ratios to determine the yields and biocrude quality that result from HTL of mixed lignocellulosic/algal feedstock. We utilize one of the most advanced mass spectrometers in existence, a custom-built 9.4 Tesla Fourier transform ion-cyclotron resonance mass spectrometer (FT-ICR MS) at the national FT-ICR user facility at the National High Magnetic Field Laboratory, to map compositional differences for HTL biocrudes generated from 100% pine, 100% algae, 75:25 pine:algae, and 50:50 pine:algae feeds. The FT-ICR MS analysis identifies thousands of compounds simultaneously within complex mixtures [13] and has been successfully applied to the analysis of HTL biocrudes from various feedstocks [5,14–21]. In general, FT-ICR MS analysis of biocrudes generated from lignocellulosic sources reveal oxygenated species (degradation of carbohydrates) are present in the highest relative abundance whereas biocrudes generated from algal sources contain higher relative abundances of nitrogen-containing species (degradation of protein) [5,14–20]. To our knowledge, this study represents the first analysis of mixed lignocellulosic/algal feeds by FT-ICR MS. Ultimately, the detailed molecular fingerprint of each mixed feed biocrude allows direct comparison of chemical composition for biocrudes derived from different feed make-up and can be used to predict and determine upgrading strategies and decipher thermochemical processes with occur during the HTL process.

2. Methods

2.1. Biocrude production

Biocrude samples were prepared using bench-scale, continuous HTL process equipment that has been previously described [2]. The 50:50 pine:algae and 100% algae tests used a system configuration with tube-in-tube plug-flow reactors only. The continuous stirred tank reactor (CSTR) was bypassed. For the 100% pine test, the CSTR was added between the preheater and main tubular reactor as insurance against plugging in the main reactor but the feed was heated to 320 °C in the tubular preheater at a high axial velocity. This was a proof-of-principle test of axial velocity as a means of preventing plugging during heating of a lignocellulosic feedstock from ambient to reaction temperature. The 75:25 pine:algae test used a configuration with a tube-in-tube reactor for feed preheating, but the reaction time at temperature was accomplished in a 1-L CSTR. The target reaction temperature for all tests was 350 °C at a pressure of 20 MPa to maintain the water in a condensed liquid phase. The biocrude samples were recovered as a gravity-separable organic phase from the largely aqueous product, no solvents were used for product recovery. Feedstock properties and HTL processing conditions are summarized in Table 1. The pine feedstock obtained from Idaho National Laboratory was a wood flour that was free of bark and branches and was milled to < 0.5 mm. *Chlorella* sp. feedstock was obtained in a dried form from Global Algae Innovations (http://www.globalgae.com). The feedstock blend ratios were calculated on dry, ash-free (daf) mass basis. The 100% pine feedstock slurry contained 1 wt% Na_2CO_3 as a buffer. The 50:50 pine:algae blend was prepared using excess pine slurry with dried algae flakes and DI water. Thus, the 50:50 pine:algae feedstock contained 0.6 wt% Na_2CO_3 in the final slurry. The 75:25 pine blend was prepared from dried pine and algal feedstock and no carbonate was added. The target concentration for dry, ash-free (daf) solids in the two blends was 15 wt%. The 100% pine feedstock solids concentration was constrained by conservative estimates of pumpability and the 100% algal feedstock concentration was prepared to meet a nominal target for algal feedstocks of 20 wt% solids (daf).

Table 1
Feedstock properties and processing conditions.

Property	Units	100% Pine	75:25 Pine:Algae	50:50 Pine:Algae	100% Algae
C	wt%	47.5%	49.4%	46.5%	47.0%
H	wt%	5.9%	6.1%	6.2%	6.6%
O	wt%	41.4%	35.3%	35.5%	27.0%
N	wt%	0.2%	2.1%	3.5%	6.3%
S	wt%	0.00%	0.20%	0.29%	0.55%
Dry solids	wt%	11.2%	15.3%	16.3%	22.1%
Ash in dry solids[a]	wt%	14.3%[a]	5.2%	9.6%	14.1%[a]
Dry, ash-free solids	wt%	9.6%	14.5%	14.7%	19.0%
Feed rate	L/h	5.985	1.500	1.995	2.042
LHSV	L/L/h	5.2	1.5	4.0	4.1
Sample Period	h	0.67	3.0	0.67	4.0
Temperature	°C	347	346	345	340
Pressure	MPa	19.9	19.4	20.5	20.4

[a] Ash in as-prepared pine feedstock is primarily added Na_2CO_3. The ash content in the pine flour is 0.65 wt% on a dry basis.

2.2. Analysis of biocrude properties

Elemental analyses for feed, liquid, and solid phases were performed using ASTM D5291/D5373 (for carbon, hydrogen and nitrogen), ASTM D5373, modified (for oxygen), and ASTM D1552/D4239 (for sulfur). In biocrude oil samples, moisture was determined by the Karl Fischer technique using Method ASTM D6869, Total Acid Number (TAN) was measured following ASTM D3339, the percentage of filtered oil solids was measured using ASTM D7579-09, and density and kinematic viscosity measurements were performed at 40 °C using an Anton Paar SVM3000 Stabinger Viscometer. Analyses for ash, dry solid content, and product weight were performed gravimetrically.

2.3. Sample preparation for FT-ICR MS

Biocrudes were dissolved in 1:1 chloroform:methanol (HPLC grade, JT Baker, Phillipsburg, NJ) to create 1 mg/mL stock solutions. Final samples were further diluted in methanol (HPLC grade, JT Baker, Phillipsburg, NJ) to 250 μg/mL with either 1% formic acid (Fluka Analytical, St. Louis, MO) for positive-ion electrospray ionization (ESI) or 0.0625% (v/v) tetramethylammonium hydroxide (TMAH) solution (25 wt% in MeOH, Acros Organics, Fair Lawn, NJ) for negative-ion ESI. For positive-ion atmospheric pressure photoionization (APPI), stock solutions were diluted to a final sample concentration of 100 μg/mL in 90:10 methanol:toluene (biocrudes).

2.4. Ionization

For electrospray ionization, a syringe pump delivered the dilute sample solutions to a microelectrospray ionization source at a rate of 0.5 μL/min. Voltage (~2 kV) was applied to the ESI needle for electrospray. Atmospheric pressure photoionization was performed with an Ion Max APPI source (ThermoFisher Corp., San Jose, CA). Samples were introduced to the source through a fused silica capillary at a rate of 50 μL/min. Nitrogen was used as a sheath gas (60 psi) and auxiliary gas (4 L/min). Inside the heated vaporizer of the source (~300 °C), the sample is mixed with a nebulization gas (N_2) and is passed under a krypton VUV lamp producing 10 eV photons (120 nm), thus allowing photoionization to occur at atmospheric pressure. Toluene was added to the samples to increase ionization efficiency through dopant-assisted photoionization.

2.5. Mass spectrometry

Samples were analyzed with a custom-built 9.4 T Fourier transform ion cyclotron resonance mass spectrometer [22]. Data collection was facilitated by a modular ICR data acquisition system (PREDATOR) [23]. Ions generated at atmospheric pressure were introduced into the mass spectrometer via a heated metal capillary. Ions were guided through the skimmer region (~2 torr) and allowed to accumulate in the first octopole (rf-only) for ESI [24]. Ions were sent through the quadrupole (mass transfer mode) to a second octopole where the ions were collisionally cooled for 1 ms with helium gas (~4–5 × 10^{-6} torr at gauge) before passage through a transfer octopole to the ICR cell (open cylindrical Penning trap [25]). For APPI, ions were allowed to pass directly through the first octopole and quadrupole for accumulation in the second octopole prior to transfer to the ICR cell.

Fifty individual time-domain transients were co-added, Hanning-apodized, zero-filled, and fast Fourier transformed prior to frequency conversion to mass-to-charge ratio [26] to obtain the final mass spectrum. For positive- and negative-ion ESI, time domain length was 7 s, which results in mass resolving power of ~1.2 M at m/z 400 in magnitude mode. For positive-ion APPI, the magnitude mode resolving power was ~8 M (m/z 400, 4.6 s time-domain transient length).

2.6. Data analysis and visualization

Data were analyzed and peak lists generated with PetroOrg© software [27]. Internal calibration of the spectrum was based on homologous series whose elemental compositions differ by integer multiples of 14.01565 Da (i.e., CH_2) [28].

Data are visualized by relative abundance histograms for heteroatom classes with a sum greater than 1% relative abundance and from isoabundance-contoured plots of double bond equivalents (DBE = number of rings plus double bonds to carbon) vs. carbon number for members of a single heteroatom class. The relative abundance scale in isoabundance-contoured plots is scaled relative to the most abundant species in that class. For APPI data, radical and protonated compounds are plotted together, with the neutral molecular formula represented and its corresponding relative abundance is a summation of the radical and protonated ions.

2.7. Multivariate statistical analysis

Principal component analyses (PCA) was performed with PetroOrg© software [27]. The deconvolution method applied was the nonlinear iterative partial least squares (NIPALS) algorithm [29]. The sum of the relative abundances for all the heteroatomic classes were entered as variables in the input data matrix. Zero-filling was applied to the matrix for missed variables [30].

3. Results and discussion

3.1. Biocrude yield, composition, and properties

Each of the HTL tests yielded gravity-separable biocrude and the overall mass balance during the sampling window ranged from 99 to 105%. Table 2 contains mass and carbon yields with associated mass balances. Reported yields are normalized to the mass balance percentage, which is computed by the mass (overall or by element) of products out divided by the mass of feed input. The highest yield is noted for the 50:50 pine:algal blend, with 0.46 g biocrude/g feed (dry, ash free). This result suggests that blends may improve overall yields to products due to the synergistic effect of amine chemistry on lignocellulosic biopolymers. Further testing is necessary to confirm the result. The solvent properties of cyclic nitrogen compounds formed from protein decomposition are well known and may lead to enhanced liquefaction of the pine feedstock [11]. In addition to enhanced liquefaction, nitrogen nucleophiles (amines, amides, imides, cyano groups) from the algal HTL processes are available to participate in condensation or substitution reactions with carbonyl or carboxyl groups from the pine feedstock and thereby increase the net mass and complexity of the formed biocrude. We discuss the observation of this type of addition, specifically of one or more nitrogen atoms added to high oxygen-containing structures, below and in the mass spectrometry results section.

Biocrude elemental compositions and properties are given in Table 3. With increased proportion of algae, the biocrude molecular oxygen content decreases while molecular nitrogen and sulfur content both increase. The viscosity and density both decrease with increasing algal content, with a significant decrease (10×) in viscosity observed between the 50:50 pine:algae blend and 100% algae biocrude. For 100% pine and both blends, the density at 40 °C is greater than 1 g/cm^3 and the biocrude was collected as the more-dense phase. Ash and filterable solids both increase as algal content increases, which corresponds to increased ash in the feedstock. The low amount of ash and

Table 3
Biocrude composition and properties.

Property	Units	100% Pine	75:25 Pine:Algae	50:50 Pine:Algae	100% Algae
Elemental compositions on a dry biocrude basis					
C	wt%	83%	82%	80%	79%
H	wt%	6.7%	8.6%	9.4%	10.6%
O	wt%	10.0%	6.3%	5.8%	3.7%
N	wt%	0.2%	2.8%	3.8%	5.5%
S	wt%	0.0%	0.2%	0.2%	0.6%
H:C ratio	mol H:mol C	0.97	1.25	1.39	1.60
$\%N_{biocrude}$:$\%N_{feed}$	ratio	1.19[a]	1.37	1.10	0.88
HHV	MJ/kg	35.9	38.1	38.5	39.6
Properties and composition on a whole (wet) biocrude basis					
TAN	mg_{KOH}/g_{oil}	53	52	56	53
Density @ 40 °C	g/cm^3	~1.10[b]	1.08	1.05	0.96
Viscosity @ 40 °C	cSt	~10,000[b]	8535	3241	295
Moisture	wt%	16.9%	6.1%	6.3%	12.0%
Ash	wt%	0.07%	0.00%	0.25%	0.47%
Filterable solids	wt%	0.04%	0.01%	0.30%	0.36%

[a] Limited significance as both biocrude and feed have low levels of nitrogen.
[b] Density and viscosity for 100% pine biocrude was not measured as high viscosity risked damage to the instrument. Values estimated from comparable historical samples.

Table 2
Biocrude mass and carbon yields normalized to mass balance.

Property	Units	100% Pine	75:25 Pine:Algae	50:50 Pine:Algae	100% Algae
Material balance and normalized yields					
Biocrude Mass Yield (N)	$g_{biocrude}/g_{feed(daf)}$	0.33	0.33	0.46	0.43
Overall Mass Balance	%	100%	105%	99%	101%
C Yield to Biocrude (N)	$g_{C,biocrude}/g_{C,feed(daf)}$	0.58	0.53	0.66	0.60
C Mass Balance	%	91%	98%	103%	106%

filterable solids in the 100% pine feedstock may be due to the added sodium carbonate as the pine feedstock was otherwise free of ash. The energy content of the fuel increases with increasing algal content as measured by the H:C ratio and the calculated HHV [31]. Evidence for the reaction of nitrogen functional groups with pine biocrude compounds may be interpreted from the ratio of biocrude nitrogen content to feedstock nitrogen content for each case. The blends have a higher biocrude nitrogen content than their feedstocks. Algal biocrude nitrogen content is 88% of that of the algal feedstock. Biller and Ross [32] reported a biocrude nitrogen/feedstock nitrogen ratio of 0.48–0.72 for four species of algae. Leow et al. [33] reported a biocrude nitrogen/feedstock nitrogen ratio 0.726 ± 0.194 for nannochloropsis cultured to have varying biochemical compositions. For algal feedstocks, the biocrude nitrogen content is found to be lower than that of the feed. Since the pine:algae blends have a biocrude nitrogen/feedstock nitrogen ratio > 1, we propose that nitrogenous compounds from the algae react with and are incorporated into compounds that are substantially derived from the liquefaction of pine.

3.2. Heteroatom distribution

Fig. 1 shows the heteroatom class distributions (> 1% relative abundance) derived from positive-ion APPI FT-ICR mass spectra of pine/algal HTL biocrude blends (i.e., 100% pine, 75:25 pine:algal, 50:50 pine:algal, and 100% algal). The pine HTL biocrude mass spectrum is dominated by O_{1-9} and N_1O_{1-7} signals whereas algal HTL biocrude nitrogen-containing compounds range from $N_{0-5}O_{0-5}$ with N > 1 present in the highest relative abundance. Pine HTL biocrude has a higher oxygen content (~10 wt%) and lower nitrogen content (< 0.2 wt%) than the algal HTL biocrude (O < 4 wt% and N > 5 wt %). For the blended feedstock oils, the heteroatom contents within these biocrudes are chiefly a composite of the parent feeds (i.e., lower oxygen and higher nitrogen content than the pine HTL biocrude and higher oxygen and lower nitrogen contents than the algal HTL biocrude (see Tables 1 and 3)) as illustrated by APPI-derived heteroatom class distributions for 75:25 and 50:50 pine:algal HTL biocrudes. Compounds observed for the 75:25 blend range from $N_{0-4}O_{0-9}$ whereas those of the 50:50 blend range from $N_{0-5}O_{0-7}$. The 75:25 blend has a higher relative abundance of nitrogen-containing compounds where N < 2 and lower relative abundance of nitrogen-containing compounds where N > 2 relative to the 50:50 blend, which is not unexpected given the nitrogen contents of the feedstocks. Additionally, all the raw biocrudes contain a low relative abundance (< 1%) of inherent hydrocarbon species due to the high heteroatom content of the feeds. The hydrocarbon content of the biocrudes can be increased through upgrading processes which generate hydrocarbon species from the abundance of heteroatom-

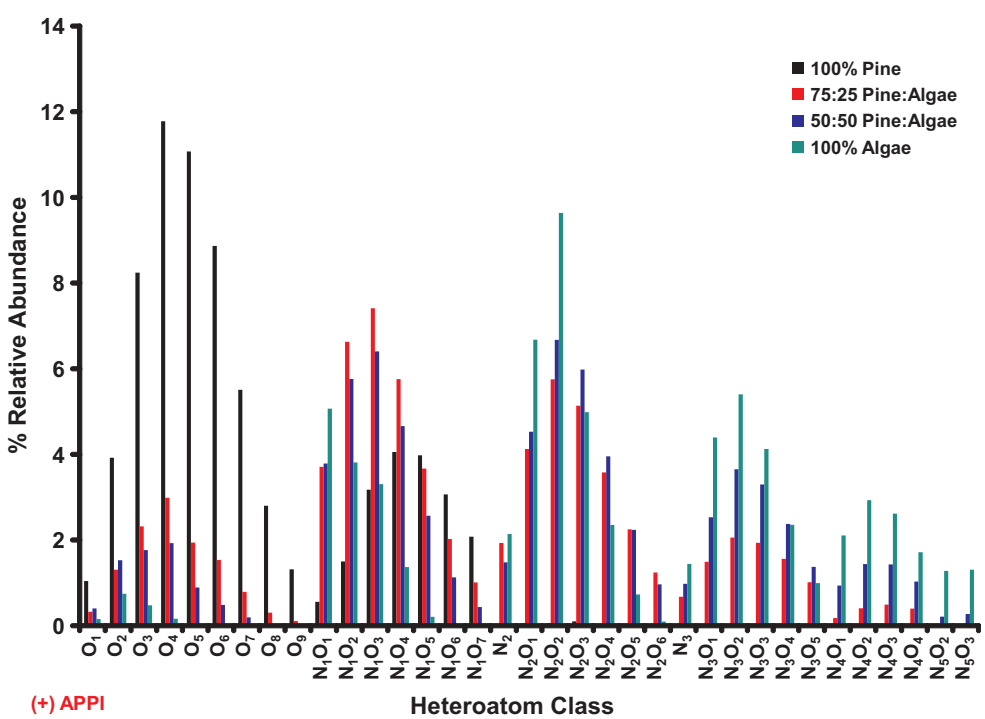

Fig. 1. Heteroatom class distributions derived from the (+) APPI mass spectra of the 100% pine (black), 75:25 pine:algal (red), 50:50 pine:algal (blue), and 100% algal (green) HTL biocrudes. (For interpretation of the references to color in this figure legend, the reader is referred to the web version of this article.)

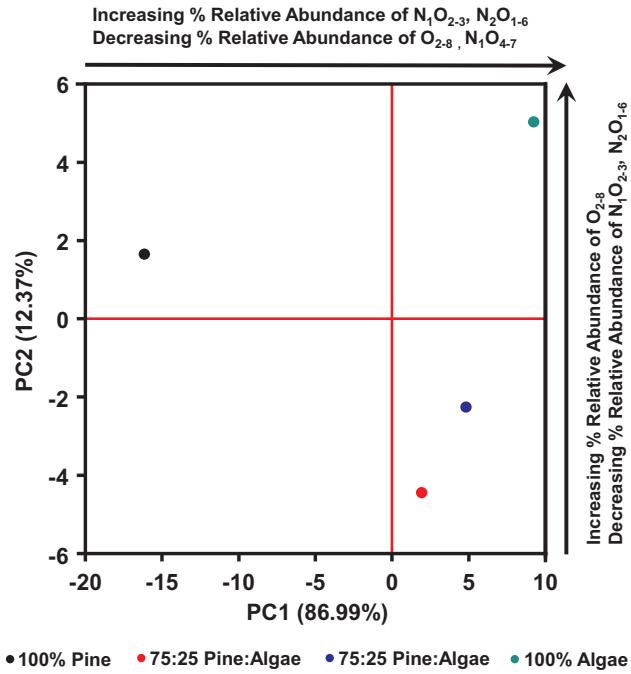

Fig. 2. Scoring plot from the PCA of the relative abundances of heteroatom classes derived from the (+) APPI mass spectra of the 100% pine (black), 75:25 pine:algal (red), 50:50 pine:algal (blue), and 100% algal (green) HTL biocrudes. (For interpretation of the references to color in this figure legend, the reader is referred to the web version of this article.)

containing species. Overall, similar trends are observed for heteroatom class distributions derived from the positive- and negative-ion ESI mass spectra of the pine/algal HTL biocrude blends (Figs. S1 and S2).

3.3. Principal component analysis

Principal component analysis (PCA) was utilized to illustrate abundance change for heteroatomic classes within the positive-ion APPI mass spectra and to establish the relationship between pure and blended feedstock biocrudes. The first and second principal components (PC1 and PC2) from this analysis account for 99.4% of the total explained variance. The score plot of PC1 vs. PC2 (Fig. 2) demonstrates the applicability of PCA to distinguish biocrude blend ratio. Note the linear correlation observed mainly for the projection presented on PC1. Biocrudes derived from feedstock with higher algal content have a higher PC1 value, while the samples with higher pine contents have a lower PC1 value. Similar to the findings of Brilman et al. [11], the mixed pine:algal feeds show a higher proportion of algal-derived materials based upon their closer proximity to the neat algal biocrude than the neat pine biocrude in PC1. Analysis of the loadings plot (Fig. S3) reveals classes that are responsible for PC1 and PC2 trends. Classes at the top, left quadrant (purple oval) are more dominant in the pine HTL biocrude whereas classes in the top, right quadrant (green oval) are more dominant in the algal HTL biocrude. Classes present in the bottom quadrants are typically more dominant in the pine:algal blended biocrude (blue oval) with the relative abundance of the classes in pine decreasing and the relative abundance of the classes in algal increasing going to the right along PC1. In general, an increase in the relative abundances of the $N_1O_{2\text{-}3}$ and $N_2O_{1\text{-}6}$ classes and a decrease in the relative abundances of the $O_{2\text{-}8}$ and $N_1O_{4\text{-}7}$ classes governs the trend in PC1, whereas PC2 is governed by the opposite trends (i.e., increase in $O_{2\text{-}8}$ and decrease in $N_1O_{2\text{-}3}$ and $N_2O_{1\text{-}6}$).

3.4. Compositional space coverage

Differences in observed compositional space between the pine/algal HTL biocrude are visualized by isoabundance-contoured plots of DBE vs. carbon number for the members of the O_3, N_1O_3, and N_2O_3 classes (positive-ion APPI mass spectra, Fig. 3). The O_3 species within the pine HTL biocrude range from $C_{11\text{-}49}$ and DBE 2-28 (outlined in red) whereas the species within the algal HTL biocrude range from $C_{16\text{-}46}$ and DBE 1-9 (outlined in green). The 75:25 and 50:50 pine:algal HTL biocrudes are a composite of the parent pine and algal HTL biocrudes with O_3 species ranging from $C_{14\text{-}37}$ and DBE 1-21 in the 75:25 blend and from $C_{14\text{-}47}$ and DBE 1-20 in the 50:50 blend. The 75:25 blend has more species in common with the pine HTL biocrude (red outline) whereas the 50:50 blend has more of the low DBE, high carbon number species from the algal HTL biocrude (green outlines). In total, the 75:25 blend has 269 and 87 O_3 species in common with the pine HTL biocrude and algal HTL biocrudes whereas the 50:50 blend has 238 and 101 O_3 species in common with the pine and algal HTL biocrudes.

Similar trends are observed for the N_1O_3 and N_2O_3 species from the pine/algal HTL biocrude blends (Fig. 3). The N_1O_3 species range from $C_{15\text{-}48}$ and DBE 1-25, $C_{13\text{-}50}$ and DBE 2-27, $C_{14\text{-}54}$ and DBE 0-25, and $C_{14\text{-}56}$ and DBE 0-17 in the pine, 75:25 blend, 50:50 blend and algal HTL biocrudes whereas the N_2O_3 species range from $C_{18\text{-}33}$ and DBE 6-16, $C_{15\text{-}57}$ and DBE 5-31, $C_{15\text{-}54}$ and DBE 2-27, and $C_{14\text{-}62}$ and DBE 0-21 in the same biocrude. In general, more algae added to the blend generates species with higher carbon numbers and lower DBE values than the species generated from the biocrude where pine is the only feedstock. Again, the 50:50 blend has more species in common with the algal HTL biocrude (green outline) than the 75:25 blend. In total, the 75:25 blend has 349 and 301 N_1O_3 species and 54 and 337 N_2O_3 species in common with the pine and algal HTL biocrudes whereas the 50:50 blend has 342 and 431 N_1O_3 species and 54 and 479 N_2O_3 species in common with the pine and algal HTL biocrudes. Because the algal HTL biocrudes contain greater average molecular nitrogen content and greater complexity, the blends tend to appear compositionally more similar to the pine HTL biocrude for species containing < 2 nitrogen atoms per molecule and more similar to the algal HTL biocrude for nitrogen-containing species where N > 1.

3.5. Monoisotopic elemental formulae analysis

The distribution of monoisotopic elemental formulae assigned to the positive-ion APPI mass spectra of pine/algal HTL biocrude blends is represented by a Venn diagram in Fig. 4. The algal HTL biocrude is the most complex (13,191 formulae) owing largely to high nitrogen and oxygen content (Table 3) which provides additional variability in composition. The pine HTL biocrude is the least complex (6,400 peaks) and the 75:25 (11,198 peaks) and 50:50 (12,713 peaks) pine:algal blends have complexities slightly lower than that the algal HTL biocrude. The composition of the 75:25 and 50:50 pine:algae biocrude blends both show a higher proportion of algal-derived species than pine-derived species – an observation that aligns with our PCA results and with the observations of Brilman et al. [11]

Interestingly, > 20% of the elemental formulae assigned to either blend are not present in either the pine or algal HTL biocrudes. The 75:25 pine:algal HTL biocrude has a higher number of elemental formulae that are not present in the parent biocrude (3044) when compared to the 50:50 pine:algal HTL biocrude (2539). Additionally, 9.2% and 4.2% of the elemental formulae assigned to the 75:25 and 50:50 blends are unique to each blend, respectively.

3.6. Novel species from pine/algal HTL biocrude blends

The 75:25 and 50:50 pine:algal HTL biocrude blends generate a large number of compounds not present in either the pine or algal HTL biocrudes. These compounds lie outside the red and green outlines in Fig.3. In the 75:25 pine:algal HTL biocrude there are 15, 90, and 182 new compounds present in the O_3, N_1O_3, and N_2O_3 classes compared to 49, 64, and 146 new compounds in the same classes from the 50:50 blend. Most of these new compounds have the similar numbers of double bonds per carbon atom as the compounds observed in pure feedstock HTL biocrudes, which suggests similar structural motifs. The blend-specific compounds are of higher DBE value and higher carbon number than those of either the pine or algal HTL biocrudes.

Fig. 5 shows detailed differences between the compositional space coverage of $N_2O_{3\text{-}6}$ classes derived from the positive-ion APPI mass spectra of the algal and pine:algal HTL biocrudes. (The pine HTL biocrude has few compounds that overlap with the algal HTL biocrude, and the pine HTL biocrude is not discussed further in this section.) The green dots represent species that are only present in the algal HTL biocrude. Gray dots represent species which are present in both the 75:25 and 50:50 blends, the red dots representing species which are present only in the 75:25 blend, and the blue dots representing species which are present only in the 50:50 blend. The number of novel compounds observed in the blend biocrudes correlates with an increase in the number of oxygen atoms. For example, the number of new species increases from 193 in the N_2O_3 class, to 230 in the N_2O_4 class, and then again to 307 in the N_2O_5 class. The number of N_2O_6 compounds in the blended feedstock biocrudes is relatively high (295), yet that class covers a less diverse compositional space than that of the algal HTL biocrude. Of the new species within the $N_2O_{3\text{-}6}$ classes, a majority of the compounds (i.e., 135, 166, 227, and 214) are common to both the 75:25 and 50:50 pine:algal blends (in gray). Both the 75:25 and 50:50 blends also have species which are unique to each blend biocrude. For a given DBE value, most of the species unique to the 50:50 blend biocrude are either one carbon number lower a few carbon numbers (< 10) higher than species observed in the algal HTL biocrude and those that are common to both blends. Additionally, the species unique to the 50:50 pine:algal HTL biocrude are not at DBE extremes and lie

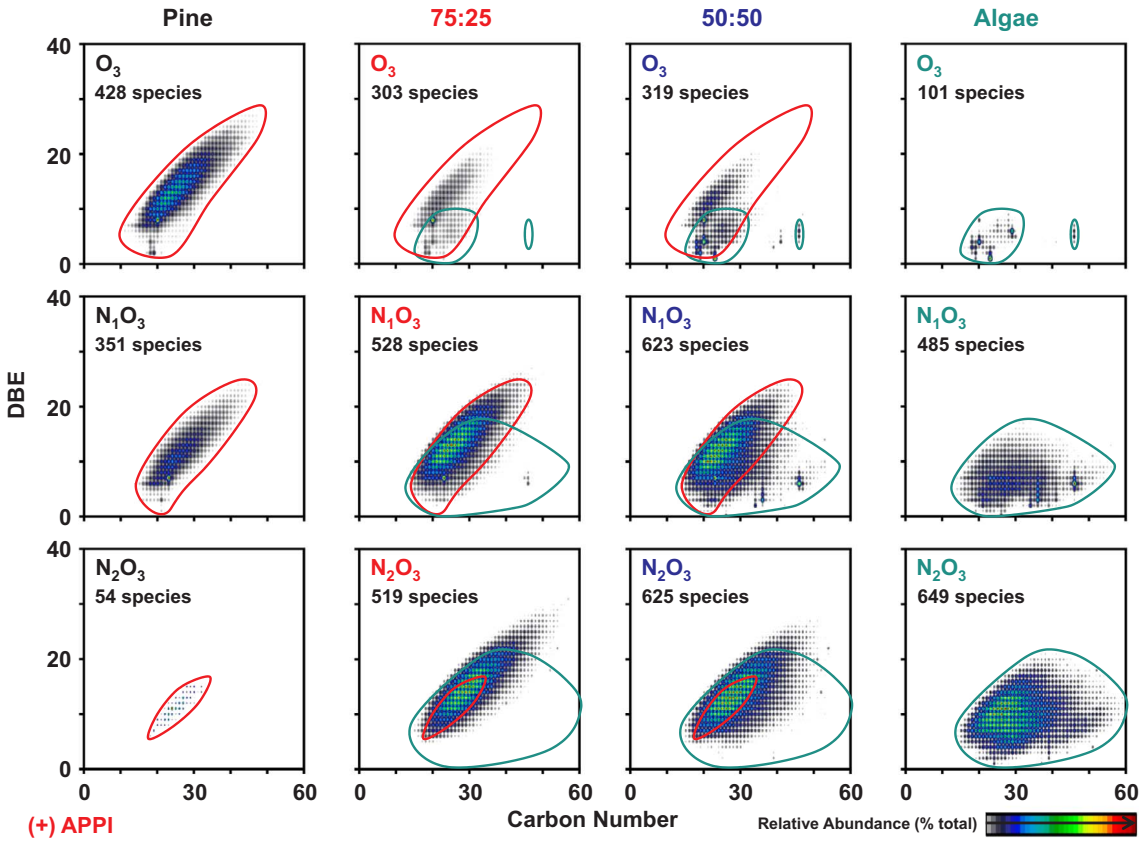

Fig. 3. Isoabundance-contoured plots of DBE versus carbon number for the O_3 (top), N_1O_3 (middle), and N_2O_3 (bottom) species derived from the (+) APPI mass spectra of the 100% pine (black), 75:25 pine:algal (red), 50:50 pine:algal (blue), and 100% algal (green) HTL biocrudes. (For interpretation of the references to color in this figure legend, the reader is referred to the web version of this article.)

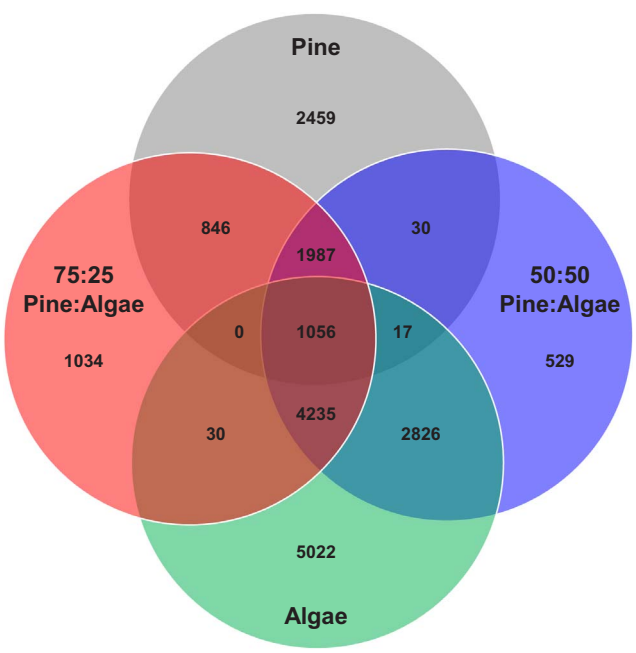

Fig. 4. Venn diagram depicting the number of monoisotopic (+) APPI molecular formulae in common between the 100% pine (top circle), 75:25 pine:algal (left circle), 50:50 pine:algal (right circle), and 100% algal (bottom circle) HTL biocrudes. There are 5 molecular formulae that are only common to the pine and algal biocrudes and 2010 molecular formulae that are only in common to the 75:25 and 50:50 pine:algal blends that cannot be visualized by the Venn diagram. Proportions are not to scale.

somewhere between DBE 10-25. In contrast, the species that are unique to the 75:25 blend are typically located at the upper right of the plots (i.e., compounds with the highest carbon number and DBE values) and have a DBE value > 25. In total, the 75:25 pine:algal blend has more unique species than the 50:50 blend due to the higher oxygen content that derives from the pine feedstock.

Fig. 6 illustrates the contribution of novel compounds observed in the 75:25 and 50:50 pine:algal blends to the total relative abundance for each class for positive-ion APPI mass spectra of the blends. The new species are members of the $O_{2\text{-}6}$, $N_1O_{1\text{-}7}$, $N_2O_{0\text{-}6}$, $N_3O_{1\text{-}5}$, and $N_4O_{2\text{-}4}$ classes. The classes which have the highest relative abundance of blend-specific species are the $N_2O_{4\text{-}6}$ and $N_3O_{4\text{-}5}$ classes where > 20% of the total abundance arises from unique to the blends. The N_2O_6 class in particular is almost entirely composed of novel species. Similar trends are observed for the new species derived from the positive- and negative-ion ESI mass spectra of the 75:25 and 50:50 pine:algal blends (Figs. S4 and S5). For example, almost all of the species within the positive-ion ESI N_2O_5 and N_3O_4 classes and the negative-ion N_1O_4 class are only generated when blending pine and algal feedstocks. Overall, the novel species are a composite of the pine and algal feedstocks, containing a median number of nitrogen atoms per molecules while incorporating more oxygen atoms per molecule from the pine feed than typically encountered in the algal HTL biocrude N_xO_y species.

4. Conclusion

FT-ICR MS analysis of the HTL biocrudes generated from pine and algal feedstocks demonstrates the composite nature of the pine/algal HTL biocrude blends as well as the formation of novel compounds compared to the pure feedstock biocrudes. Both the 75:25 and 50:50 pine:algal HTL biocrudes contain heteroatom classes with lower

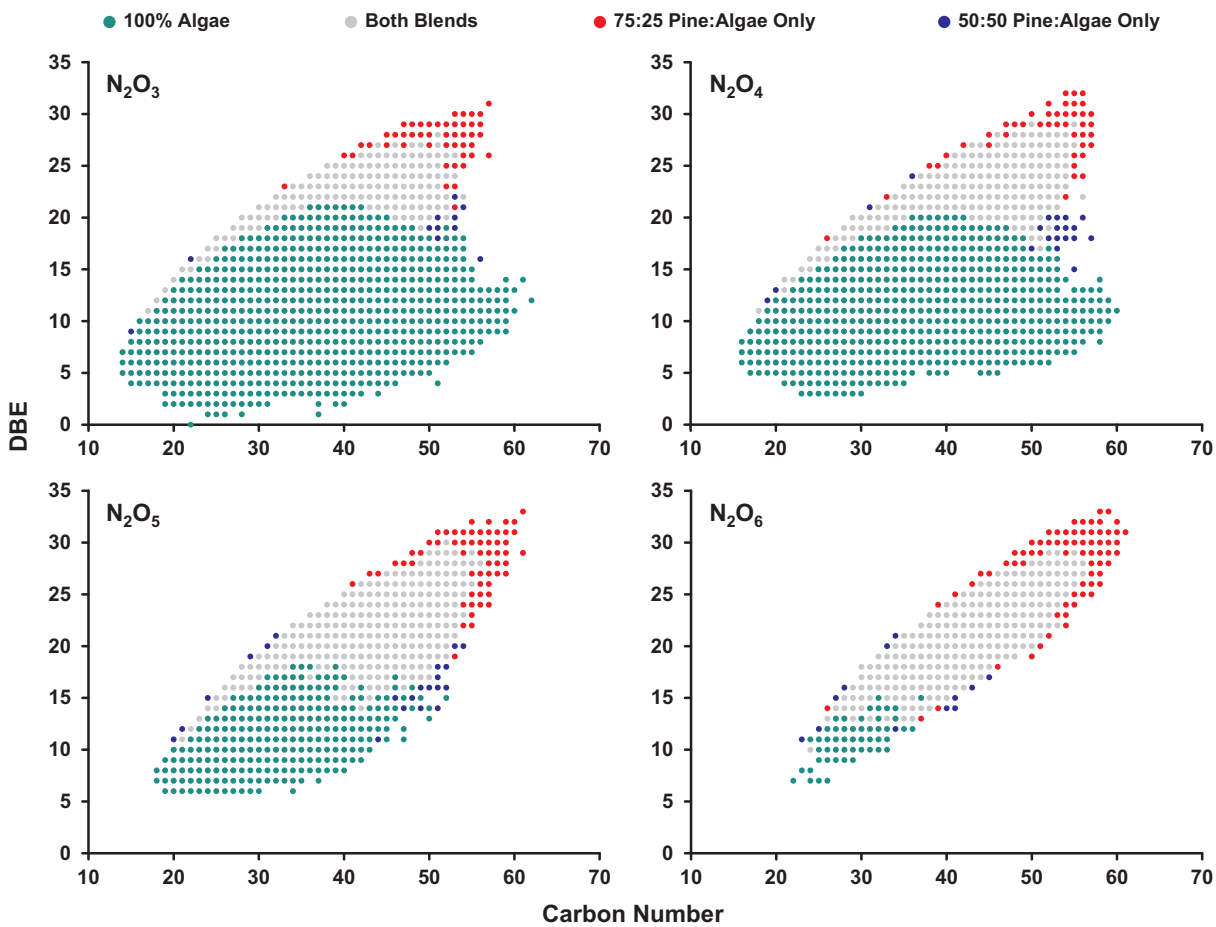

Fig. 5. Composite plots of DBE versus carbon number for the N_2O_3 (top, left), N_2O_4 (top, right), N_2O_5 (bottom, left), and N_2O_6 (bottom, right) species derived from the (+) APPI mass spectra of the 75:25 pine:algal, 50:50 pine:algal, and 100% algal HTL biocrudes. Species present in the algal HTL biocrude (green), common to both the 75:25 and 50:50 blends (gray), and unique to the 75:25 (red) or 50:50 (blue) are shown. (For interpretation of the references to color in this figure legend, the reader is referred to the web version of this article.)

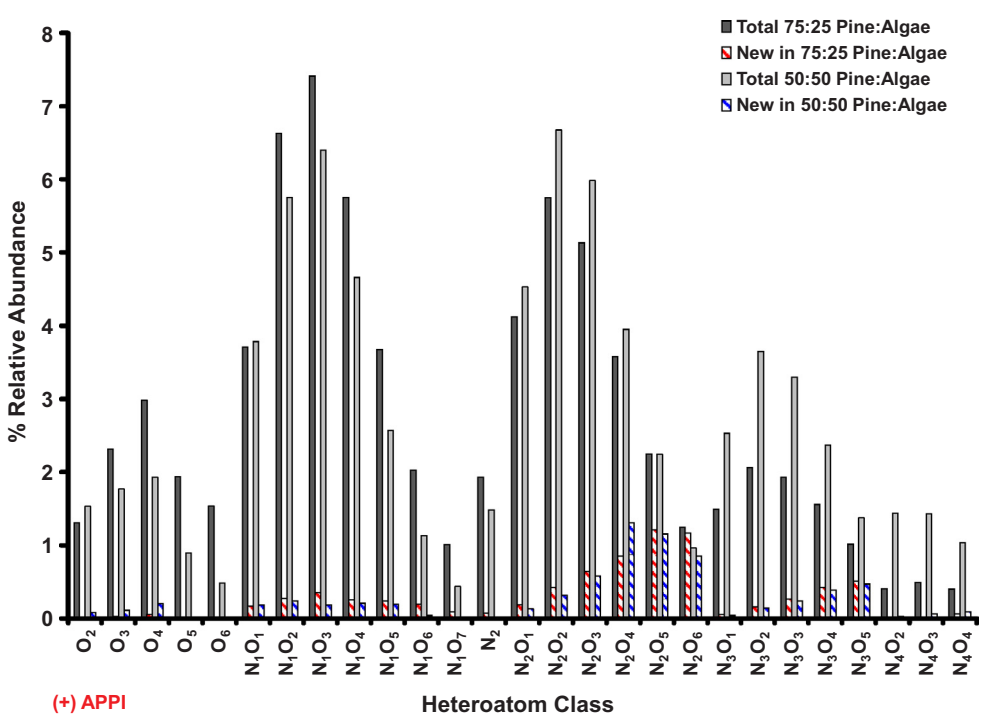

Fig. 6. Heteroatom class distributions derived from all the species present in (+) APPI mass spectra of the 75:25 pine:algal (dark gray) and 50:50 pine:algal (light gray) and species present in only the 75:25 (red strip) and 50:50 (blue strip) pine:algal HTL biocrudes. (For interpretation of the references to color in this figure legend, the reader is referred to the web version of this article.)

oxygen/higher nitrogen contents than the pine HTL biocrude and higher oxygen/lower nitrogen contents than the algal HTL biocrude. Compositionally, the blends tend to appear more similar to the pine HTL biocrude for species containing < 2 nitrogen atoms per molecule and more similar to the algal HTL biocrude for nitrogen-containing species where N > 1. Both pine:algae biocrude blends show a higher than expected proportion of species in common with the algal-derived biocrude versus the pine-derived biocrude, as noted in previous studies [11].

Simultaneous liquefaction of pine and algal feedstocks generates novel species which are an amalgamation of the pine and algal feedstocks, containing a median number of nitrogen atoms per molecules while incorporating more oxygen atoms per molecule from the pine feed than typically encountered in the pure algal HTL biocrude. These new species have more aromatic character, but a similar structural motif, as the compounds from the biocrudes generated from the pure feeds. Ultimately, the 75:25 pine:algal blend has more unique species due to the higher portion of pine feed, which allows for the incorporation of more oxygen character into a variety of nitrogen-containing compounds derived from the algal feed.

Ultimately, the HTL biocrudes from mixed feeds have been shown to be characteristically similar to biocrudes generated from each unadulterated feed and an economically viable option to increase HTL production. In fact, several advantages of the pine/algal HTL biocrudes were also discovered. Lignocellulosic HTL products typically have an acidic pH (i.e., 4–5.4) due to the hydrothermal reactions of cellulose and hemicellulose that generate organic acids (e.g., formic and acetic acid) [1,34]. The acidic conditions generated during HTL of lignocellulosic biomass can lead to detrimental effects such as corrosion or polymerization [34,35]. Therefore, Na_2CO_3 is often added into lignocellulosic slurries prior to HTL to help buffer the pH and keep it from going below 4, but often results in high Na concentrations in the HTL products [34]. However, the pH of microalgal-derived HTL products is typically basic (i.e., pH 7–9) [36] with nitrogenous compounds acting as a buffer that elevates pH and counters the presence of organic acids [2,36]. The addition of algal to lignocellulosic feedstocks generates products which are naturally more buffered to against pH extremes and eliminates the need for Na_2CO_3 buffers.

Additionally, blending lignocellulosic feeds with algal feeds can also help reduce some of the more detrimental effects due to the higher nitrogen, sulfur, and trace metal contents of microalgal feeds. High nitrogen and sulfur contents can lead to harmful NO_x and SO_x emissions, and have to be removed during upgrading [1,2], whereas trace metals in microalgal have also been shown to cause problems during upgrading of microalgal-derived HTL biocrudes [37]. Lignocellulosic feeds have been shown to have lower nitrogen, sulfur, and trace metal contents, which can decrease the impact of these harmful heteroatoms during HTL and upgrading processes.

Acknowledgments

This work was supported by the U.S. Department of Energy's Office of Energy Efficiency and Renewable Energy (Bioenergy Technologies Office), the United States National Science Foundation (IIA-1301346 and MRI-1626468), the Center for Animal Health and Food Safety at New Mexico State University, and NSF Division of Materials Research (DMR-11-57490). The authors thank the ICR staff at National High Magnetic Field for their help with instrument set-up and data collection.

Appendix A. Supplementary data

Supplementary data associated with this article can be found, in the online version, at http://dx.doi.org/10.1016/j.fuel.2017.12.016.

References

[1] Elliott DC, Biller P, Ross AB, Schmidt AJ, Jones SB. Bioresour Technol 2015;178:147–56.
[2] Elliott DC, Hart TR, Schmidt AJ, Neuenschwander GG, Rotness LJ, Olarte MV, et al. Algal Res 2013;2(4):445–54.
[3] Davis RE, Fishman DB, Frank ED, Johnson MC, Jones SB, Kinchin CM, et al. Environ Sci Technol 2014;48(10):6035–42.
[4] Biddy M, Davis R, Jones S, Zhu Y. Whole Algae Hydrothermal Liquefaction Technology Pathway: Technical Report NREL/TP-5100-58051; PNNL-22314 Washington, D.C.: U.S. Dept. of Energy; 2013.
[5] Jarvis JM, Billing JM, Hallen RT, Schmidt AJ, Schaub TM. Energy Fuels 2017.
[6] Hossain FM, Rainey TJ, Ristovski Z, Brown RJ. Renew Sustain Energy Rev 2017.
[7] Lavanya M, Meenakshisundaram A, Renganathan S, Chinnasamy S, Lewis DM, Nallasivam J, et al. Bioresour Technol 2016;203(Supplement C):228–35.
[8] Gerber LN, Tester JW, Beal CM, Huntley ME, Sills DL. Environ Sci Technol 2016;50(7):3333–41.
[9] Jones SB, Zhu Y, Anderson DB, Hallen RT, Elliott DC, Schmidt AJ, et al. Process Design and Economics for the Conversion of Algal Biomass to Hydrocarbons: Whole Algae Hydrothermal Liquefaction and Upgrading. 2014. Richland, WA.
[10] Chen WT, Zhang Y, Zhang J, Schideman L, Yu G, Zhang P, et al. Appl Energy 2014;128:209–16.
[11] Brilman DWF, Drabik N, Wądrzyk M. Biomass Convers Biorefinery 2017:1–10.
[12] Madsen RB, Bernberg RZK, Biller P, Becker J, Iversen BB, Glasius M. Sustain Energy Fuels 2017;1(4):789–805.
[13] Marshall AG, Rodgers RP. Acc Chem Res 2004;37(1):53–9.
[14] Faeth JL, Jarvis JM, McKenna AM, Savage PE. AIChE J 2015.
[15] Sudasinghe N, Dungan B, Lammers P, Albrecht K, Elliott D, Hallen R, et al. Fuel 2014;119:47–56.
[16] Sudasinghe N, Cort JR, Hallen R, Olarte M, Schmidt A, Schaub T. Fuel 2014;137:60–9.
[17] Sanguineti MM, Hourani N, Witt M, Sarathy SM, Thomsen L, Kuhnert N. Algal Res 2015;9:227–35.
[18] Cheng F, Cui Z, Chen L, Jarvis J, Paz N, Schaub T, et al. Appl Energy 2017;206(Supplement C):278–92.
[19] Dandamudi KPR, Muppaneni T, Sudasinghe N, Schaub T, Holguin FO, Lammers PJ, et al. Bioresour Technol 2017;236(Supplement C):129–37.
[20] Zhang J, Qian C, Jiang B. J Agric Saf Health 2017.
[21] Kostyukevich Y, Vlaskin M, Borisova L, Zherebker A, Perminova I, Kononikhin A, et al. Eur J Mass Spectrom 2017. 1469066717737904.
[22] Kaiser NK, Quinn JP, Blakney GT, Hendrickson CL, Marshall AG. J Am Soc Mass Spectrom 2011;22:1343–51.
[23] Blakney GT, Hendrickson CL, Marshall AG. Int J Mass Spectrom 2011;306(306):246–52.
[24] Senko MW, Hendrickson CL, Emmett MR, Shi SD-H, Marshall AG. J Am Soc Mass Spectrom 1997;8:970–6.
[25] Kaiser NK, Savory JJ, McKenna AM, Quinn JP, Hendrickson CL, Marshall AG. Anal Chem 2011;83:6907–10.
[26] Ledford Jr. EB, Rempel DL, Gross ML. Anal Chem 1984;56:2744–8.
[27] Corilo, Y. E. PetroOrg Software. Florida State University. All rights reserved. www.petroorg.com.
[28] Kendrick E. Anal Chem 1963;35:2146–54.
[29] Esbensen K. Multivariate Analysis – In Practice. 3rd ed. Trondheim, Norway: CAMO; 1998.
[30] Lohninger H. Teach/Me Data Analysis. Berlin-New York-Tokyo: Springer; 1999.
[31] Channiwala SA, Parikh PP. Fuel 2002;81(8):1051–63.
[32] Biller P, Ross AB. Bioresour Technol 2011;102(1):215–25.
[33] Leow S, Witter JR, Vardon DR, Sharma BK, Guest JS, Strathmann TJ. Green Chem 2015;17(6):3584–99.
[34] Panisko E, Wietsma T, Lemmon T, Albrecht K, Howe D. Biomass Bioenergy 2015;74:162–71.
[35] Toor SS, Rosendahl L, Rudolf A. Energy 2011;36(5):2328–42.
[36] Maddi B, Panisko E, Wietsma T, Lemmon T, Swita M, Albrecht K, et al. Biomass Bioenergy 2016;93:122–30.
[37] Jarvis JM, Sudasinghe NM, Albrecht KO, Schmidt AJ, Hallen RT, Anderson DB, et al. Fuel 2016;182:411–8.